Published in final edited form as:
Skeletal Radiol. 2012 April ; 41(4): 437–445. doi:10.1007/s00256-011-1240-1.

LOWER LEG MUSCLE INVOLVEMENT IN DUCHENNE MUSCULAR DYSTROPHY: AN MR IMAGING AND SPECTROSCOPY STUDY

Martin Torriani, M.D., M.Sc.[1], **Elise Townsend, D.P.T, Ph.D.**[2], **Miriam A. Bredella, M.D.**[1], **Bijoy J. Thomas, M.D.**[1], **Reza Hosseini Ghomi, M.S.E.**[1], and **Brian S. Tseng, M.D., Ph.D.**[3]

[1]Division of Musculoskeletal Imaging and Intervention, Massachusetts General Hospital and Harvard Medical School, Boston, MA

[2]MGH Institute of Health Professions and Massachusetts General Hospital, Boston, MA

[3]Pediatric Neuromuscular Clinic, Massachusetts General Hospital and Harvard Medical School, Boston, MA and Novartis Institute of Biomedical Research, Cambridge MA

INTRODUCTION

Duchenne muscular dystrophy (DMD) is an incurable recessive X-linked disease of childhood and the most common pediatric muscular dystrophy, affecting 1 in every 4,000 male births [1]. The disease is caused by loss-of-function mutations in the gene dystrophin located on the X chromosome (Xp21), which codes for the protein dystrophin, an important structural component of muscle. This abnormality results in structural fragility, membrane permeability, metabolic crisis and progressive myocyte degeneration. Boys with DMD suffer progressive loss of strength and function that lead to wheelchair dependence, cardiorespiratory compromise, and eventually death during young adulthood [1].

Muscle involvement in DMD is characterized by repetitive cycles of injury, inflammation and repair that result in progressive necrosis and replacement of muscle cells by fat and fibrous tissue [2]. One of the hallmarks of muscle involvement in DMD is a significant loss of muscle bulk in the proximal musculature, including those of pelvis and thighs. Prior imaging studies of pelvic and thigh muscles in DMD subjects have shown a characteristic pattern of fatty infiltration that spares the gracilis, sartorius, and semi-membranosus muscles [2–5]. Furthermore, the degree of adiposity of pelvic and thigh muscles measured by MR imaging correlated with clinical functional indices, serving as quantitative and objective measures of disease severity [2, 6].

Lower leg muscles, in particular the posterior compartment, paradoxically show an enlarged appearance known as pseudohypertrophy, which is characteristic however not specific of DMD [7]. The tissue transformation of posterior lower leg musculature is associated with loss of plantar flexor muscle length, which leads to the characteristic toe-walking gait pattern seen in boys with DMD in the later ambulatory stage of disease progression. Although objective evidence confirms lower leg enlargement in boys with DMD, clinical perception is affected by body weight, height and atrophy of proximal muscles [7]. While MR imaging studies of muscular dystrophies have focused on quantitative methods measuring pelvic and thigh muscle involvement, such data regarding lower leg musculature

CORRESPONDING AUTHOR: Martin Torriani, M.D., M.Sc., Musculoskeletal Imaging and Intervention, Department of Radiology, Massachusetts General Hospital, 55 Fruit Street – YAW 6048 – Boston, MA – 02114, Phone: 617-724-1108 – Fax: 617-726-5282, mtorriani@hms.harvard.edu.

are limited. Only one prior study specifically addressed lower leg muscles using MR imaging T2 mapping, showing correlation with disease severity [5], whereas other imaging-based studies either employed only qualitative assessments [3, 4] or did not specifically evaluate boys with DMD [8, 9]. Importantly, no prior studies have described the precise pattern of fatty infiltration of lower leg muscles by MR imaging in DMD, nor are there objective measures of tissue-level changes using 1H- and 31P-MR spectroscopy. Furthermore, the value of such measures as surrogates for disease severity is unknown. Since lower leg muscles have a distinct clinical appearance as DMD progresses and retain function longer than their proximal counterparts, a better understanding of its changes may have potentially important implications in monitoring long term therapies.

Therefore, the purpose of our study was to detail the involvement of lower leg muscles in DMD using MR imaging and spectroscopy and provide non-invasive biomarkers of functional status in boys with DMD. We performed lower leg muscle MR imaging, 1H- and 31P-MR spectroscopy in subjects with DMD compared to age- and BMI-matched healthy controls. We also aimed to investigate the relationships between our data and clinical indices of muscle strength and function in children with DMD.

MATERIALS AND METHODS

This study was approved by the Institutional Review Board and complied with HIPPA guidelines. Written informed consent was obtained from all subjects, parents or guardians prior to enrollment.

Subjects

We prospectively recruited two groups. One group included boys with DMD (DMD group) and the other group comprised age- and BMI-matched healthy control boys (control group). Both groups were recruited either from our institution's Pediatric Neuromuscular Clinic or from the community at large. Inclusion criteria for the DMD group were: male subjects older than 7 years of age (age cut-off chosen to increase likelihood of cooperation during MR examination without need for sedation); previously diagnosed DMD at any stage documented by clinical exam, DNA mutation analysis, serum creatine kinase, and/or muscle biopsy results; and cognitively able to follow instructions and give assent. Age- and BMI-matched male healthy controls were not taking prescribed medications and had no history of disease known to affect muscle metabolism. Exclusion criteria for both groups included presence of metallic orthopedic hardware in the lower extremity that could affect MR measurements, routine MR imaging exclusion criteria, and inability to cooperate during MR examination. Boys in the DMD group were evaluated clinically for history of muscle weakness, changes in weight, diet, activity level, medications and use of dietary supplements. The physical exam included height, weight, and BMI calculations. The clinical stage of DMD was evaluated using the 10-point lower extremity functional rating scale described by Vignos et al. [10] (Table 1). A higher score on this scale indicates lower muscle function.

MR imaging data acquisition

All imaging was performed using a 3.0T (Siemens Trio; Siemens Medical Systems, Erlangen, Germany) system. For 1H-MR imaging and spectroscopy acquisitions, subjects were scanned while positioned feet first in the magnet bore with the right lower leg placed in a commercially available 12-element transmit/receive quadrature extremity coil, with 18 cm diameter (USA Instruments, Aurora, Ohio). A tri-plane gradient echo localizer pulse sequence with echo time (TE) of 5 ms and repetition time (TR) of 15 ms was obtained. Axial T1-weighted images (TR, 400 ms; TE, 11 ms; slice thickness, 4 mm; inter-slice gap, 1

mm; matrix, 512 × 512; NEX, 1; FOV 22 cm) of the proximal two-thirds of the lower leg were obtained using the proximal tip of the fibula as an osseous landmark. The first slice was placed at the level of proximal fibular tip and the prescription stack was propagated distally with the above-mentioned thickness and spacing parameters.

MR imaging data analysis

Fatty infiltration of the lower leg musculature was graded using semi-quantitative and quantitative methods. The semi-quantitative method entailed consensus scoring by two radiologists blinded to patient data to minimize bias. The muscles analyzed were: tibialis anterior, tibialis posterior, extensor digitorum longus, peroneals (brevis and longus analyzed as a unit), medial head of gastrocnemius, and lateral head of gastrocnemius. At the largest cross-sectional area of each muscle, we used the scale described by Kim et al. [2], as follows: grade 0, homogeneous muscle signal intensity without fatty infiltration; grade 1 (minimal), predominantly homogeneous muscle signal intensity with minimal scattered fatty infiltration (often seen in soleus muscle); grade 2 (mild), mild fatty infiltration with additional patchy areas of intramuscular high T1 signal intensity involving less than 30% of muscle bulk; grade 3 (moderate), moderate fatty infiltration involving 30%–60% of muscle bulk, and preserved differentiation between muscle and subcutaneous fat; and grade 4 (severe), severe fatty infiltration involving more than 60% of muscle bulk with loss of demarcation between muscle and subcutaneous fat. A cumulative score for each muscle was obtained separately for the DMD and control groups.

Quantitative measures of muscle fatty infiltration were obtained by determining the amount of intra-muscular adipose tissue (IMAT) [11]. In all subjects, a single axial T1-weighted image was selected 10 cm distal to the fibular tip, and the total cross-sectional area of the lower leg muscles was determined (Osirix version 3.8.1, http://www.osirix-viewer.com/index.html). Next, pixel values corresponding to muscle were manually segmented (ViTrak, Merge/Efilm, WI), providing an area that was subtracted from the total muscle cross-sectional area. This yielded an estimate of IMAT, which was normalized to total muscle cross-sectional area to account for variability in lower leg sizes.

1H- and 31P-MR spectroscopy data acquisition

Single-voxel 1H-MRS data was acquired using point-resolved spatially localized spectroscopy (PRESS) pulse sequence with a TE of 30 ms, TR of 3,000 ms, 64 acquisitions, 1024 data points, and receiver bandwidth of 1000 Hz. The PRESS acquisition time lasted 3 minutes and 24 seconds. In all cases, a voxel measuring 12 × 12 × 12 mm (1.7 mL) was placed on the axial T1-weighted slice with largest muscle cross-sectional area of the tibialis anterior (TA) and the soleus (SOL) muscles, avoiding visible fat or vessels. Water presaturation was used for metabolite acquisition, and unsuppressed water spectra of same voxel were obtained for each scan (same parameters as above, however using 8 acquisitions). For each voxel placement, we performed automated optimization of gradient shimming, water suppression, and transmit-receive gain, followed by manual shimming targeting linewidths of 10–12 Hz.

Non-localized 31P-MRS was performed immediately following 1H-MRS acquisitions using the same MR system described above. A 13-cm-diameter custom-built single-tuned 31P surface coil was placed in contact with the anterior and subsequently posterior lower leg muscles. 31P spectra from both compartments were acquired from the resting muscles (TR, 1,500 ms; TE, 0.225 ms; 128 averages; bandwidth: 2,000 Hz; flip angle: 90 degrees). Dynamic 31P-MRS studies were not performed due to time constraints and to avoid negative effects on functional measures performed immediately after MR spectroscopy acquisitions.

1H- and 31P-MR spectroscopy data analysis

Fitting of 1H-MRS metabolite data was performed using LCModel (version 6.2-2B) [12]. Data were transferred from the MR scanner to a Linux workstation and metabolite quantification was performed using water scaling based on unsuppressed water peak (4.7 ppm). The fitting algorithm was customized for muscle analysis and provided a combined estimate for lipid peaks (0.9, 1.1, 1.3, 1.5, 2.1 and 2.3 ppm). This combined estimate was multiplied by 100 and expressed as the lipid fraction of muscle. Due to the potential effect of different muscle water concentrations between groups, we also measured the concentration of unsuppressed water within each voxel using the Hankel-Lanczos single-variable decomposition (HLSVD) fitting algorithm in jMRUI software (version 4.0) [13]. Phosphocreatine (PCr), inorganic phosphate (Pi), and adenosine triphosphate (ATP) resonances were fitted in the time domain using the AMARES routine in jMRUI. Relative PCr and Pi concentrations were calculated using the β-ATP resonance as reference. Intracellular pH was estimated based on the chemical shift difference between PCr and Pi resonances [14].

Clinical motor assessments

Timed functional motor tests typically employed in muscular dystrophy clinical trials were performed for subjects in the DMD group and included a six-minute walk test (distance covered in 6 minutes on a 20 m course) [15], a timed 10 meter walk (time to walk a 10 m course), time to climb 4 stairs and time to rise from the floor [16]. All functional testing was performed on the same day and immediately after MR imaging and spectroscopy procedures by a single physical therapist experienced in standardized testing of boys with DMD.

Statistical analyses

Statistical analyses were performed using JMP Statistical Database Software (SAS Institute, Inc., Cary, NC). Data are expressed as means ± standard deviation and statistical significance was set at $P < 0.05$. Normal distribution of data was evaluated using Shapiro-Wilk W test and data not normally distributed were log transformed before statistical analyses. This was required for TA and SOL lipid fraction. To account for the possibility of muscle edema in DMD subjects and its potential effect in 1H-MRS ratios, an analysis of covariance (ANCOVA) was used to determine differences of 1H-MRS lipid fractions between groups controlling for the concentration of unsuppressed water. Student's *t* tests were used to analyze mean differences of 31P-MRS variables between the two groups. Pearson correlation coefficients were calculated to explore associations among MRS and clinical motor variables for normally distributed data and, after logarithmic transformation, of data for variables not normally distributed.

RESULTS

Subjects

A total of 17 subjects (n = 9, DMD group; n = 8, control group) were recruited and tested. Mean age of the DMD group was 11 ± 3.4 years (range, 8 to 18 years) and mean body mass index (BMI) was 22 ± 8 kg/m^2 (range, 13 – 40). The mean age of the control group was 13 ± 2.5 years (range, 10 – 17) and mean BMI was 24 ± 5 kg/m^2 (range, 16 – 30). No significant difference in age ($P = 0.2$) or BMI ($P = 0.6$) was found between groups. The mean Vignos lower extremity functional rating of DMD subjects was 4 (range, 2 to 8). One subject with DMD was not available for functional motor testing and another was non-ambulatory, and unable to complete motor testing.

MR imaging data in DMD vs. control group

In both DMD and control groups, the peroneal muscles showed the greatest fatty infiltration cumulative score of all lower leg muscle groups (scores 20 and 9, respectively), whereas the tibialis posterior muscle showed the lowest cumulative score (scores 4 and 4, respectively) (Figure 1). The fatty infiltration grades of lower leg muscles in both groups are outlined in Figure 2. Despite overall higher cumulative fatty infiltration scores in DMD compared to control subjects, only SOL had a significantly higher score in the DMD group compared to the control group (17 vs. 5, $P = 0.01$). DMD subjects had significantly higher normalized IMAT when compared to control subjects (Table 1). No significant difference in lower leg total cross sectional area was found between DMD and control groups, either before or after controlling for age ($P = 0.2$ and 0.6, respectively).

1H- and 31P-MR spectroscopy data in DMD vs. control group

All subjects successfully completed the proposed MR data acquisitions. Means and standard deviations of 1H- and 31P-MRS parameters for both study groups are outlined in Table 2. Overall, the DMD group had significantly higher lipid fraction within the TA and SOL compared to the control group. The unsuppressed water concentration was significantly higher in SOL of the DMD group ($P = 0.01$), however was not significantly different between groups for TA ($P = 0.31$). The DMD group had significantly higher pH of anterior lower leg muscles, and significantly lower PCr/Pi ratio of posterior lower leg muscles.

Relationships between clinical motor abilities, functional rating and lower leg muscle MR data

The Vignos lower extremity functional ratings correlated with 1H-MRS measures of TA lipid fraction (r = 0.79, P = 0.01) and SOL lipid fraction (r = 0.71, P = 0.03). Walking endurance as indexed by distance covered in a six-minute walk test was inversely correlated with MR imaging fatty infiltration scores of SOL (r = −0.76, P = 0.046), medial head of gastrocnemius (r = −0.80, P = 0.03), lateral head of gastrocnemius (r = −0.84, P = 0.02), as well as with normalized lower leg IMAT (r = −0.80, P = 0.03) and SOL lipid fraction (r = −0.89, P = 0.01). Time to walk 10 meters was positively correlated with 31P-MRS measures of anterior lower leg pH (r = 0.78, P = 0.04) and showed a positive trend with normalized lower leg IMAT (r = 0.73, P = 0.06). The remaining MRI, MRS and clinical parameters were not significantly correlated (P > 0.05).

Correlations between the different muscle adiposity measurements were also examined. Positive correlations were present between 1H-MRS lipid fraction and MR imaging fatty infiltration scores of TA ($r = 0.77$, $P = 0.0003$) and SOL ($r = 0.94$, $P < 0.0001$), which persisted in separate sub-analysis of the DMD group alone (TA: $r = 0.72$, $P = 0.03$; SOL: $r = 0.94$, $P = 0.0002$). 1H-MRS lipid fractions also correlated strongly with normalized IMAT in both groups (TA: $r = 0.67$, $P = 0.003$; SOL: $r = 0.92$, $P < 0.0001$). In sub-analysis of the DMD group, only SOL lipid fraction correlated with normalized IMAT ($r = 0.90$, $P = 0.001$).

DISCUSSION

There is increasing evidence that quantitative methods to determine muscle fat accumulation play an important role in predicting the progression of DMD [2, 6]. The majority of this research has focused on pelvic and thigh muscles, which are involved in early disease stages. Although thigh muscles of children with DMD tend to decrease in volume after the age of 7 years due to fiber atrophy [7, 17], lower leg muscles frequently show enlargement as the disease progresses, a phenomenon known as pseudohypertrophy. Beenakker et al. [7] showed significantly increased lower leg circumference in ambulatory children with DMD

compared to weight-matched healthy controls, confirming that pseudohypertrophy was not due to relative decrease of thigh circumference. Although histologic evidence of scattered hypertrophied muscle fibers in lower leg muscle needle biopsy samples of DMD patients has been reported [18], pseudohypertrophy occurs predominantly as a function of fat and fibrous tissue accumulation that is 2 to 3 times higher when compared to healthy controls [17]. The cause for this unique behavior remains unknown, however profiling the metabolism of lower leg muscles may provide important information regarding the progression of DMD, because of the delayed involvement of these muscles. Importantly, no prior studies have concurrently examined the relationship between MR imaging, 1H- and 31P-MRS data of lower leg musculature and clinical indices of functional motor status in DMD. Furthermore, establishing the imaging characteristics of lower leg muscles in DMD may be useful to evaluate the disease in advanced stages, in which thigh and pelvic muscles are severely infiltrated with fat and most muscle cells are destroyed.

In our study, MR imaging scores of fatty infiltration in children with DMD revealed an atrophy pattern that affected predominantly the peroneal, gastrocnemius and soleus muscles. While the marked involvement of peroneal muscles was a characteristic feature in our cohort of boys with DMD, only the soleus muscle had significantly higher fatty infiltration scores when compared to healthy controls. In a qualitative MR imaging study using cross-sections of the pelvis, thighs and calves in DMD patients, Schreiber et al. [3] observed fatty infiltration of the lower leg muscles that was more prominent posteriorly. Although not specifically discussed, the authors provided an image of a 10.5 year-old boy with DMD that showed predominant fatty infiltration of the peroneal muscles bilaterally [3]. Prior studies have reported selective sparing of gracilis, sartorius and semi-membranosus muscles in DMD [2–4, 6, 19]. Similarly, our study showed the tibialis posterior muscle had normal appearance even in the most severe cases. In a prior study, negative correlations between mean computed tomography attenuation values and age for peroneus, soleus and gastrocnemius muscles were noted, however the tibialis posterior and anterior showed no significant age-related changes in attenuation and remained preserved up to relatively advanced ages [20]. The underlying etiology of selective muscle involvement and sparing in the proximal and distal lower extremity is uncertain. However, Marden et al. [19] noted hypertrophy of gracilis and sartorius muscles in boys with more advanced fatty infiltration, suggesting dystrophy-resistant muscles may undergo compensatory enlargement. In our cohort of DMD children, we did not observe compensatory hypertrophy of preserved muscles, such as the tibialis posterior, extensor digitorum longus and tibialis anterior.

In a recent study, Kim et al. [2] showed that T2 maps of the pelvic and thigh muscles served as quantitative and objective measures of disease severity, with significant correlations between T2 values and MR imaging scores of fatty infiltration. Furthermore, positive correlations between T2 values of gluteus maximus muscle and age, clinical functional score, Gowers score, and time to run 10 m were present [2]. In another study using the three-point-Dixon MR imaging technique, strong correlations were found between fat percentage of thigh muscles, age and functional grade, whereas no significant correlations were noted between functional grade and manual muscle testing or dynamometer strength measures [6]. Taken together, these results suggest that MR imaging can assess disease status by objectively measuring pelvic and thigh muscle atrophy.

Quantitative MR imaging and 1H-MRS data of lower leg muscles from our study also suggest a clear relationship between increased muscle adiposity and decreased muscle function in DMD patients. We observed that lipid fractions from TA and SOL were significantly increased in DMD compared to healthy children, and strongly correlated with the Vignos lower extremity functional ratings. These findings are in line with prior observations in which increased fat content in pelvis and thigh muscles of DMD children

were considered reliable markers of disease progression [2, 6]. Furthermore, correlations among the several methods we used to determine lower leg muscle adiposity in our study suggest both quantitative and semi-quantitative techniques can reliably provide indices that are associated with disease stage.

In boys with DMD, compensatory gait patterns, including toe-walking, are a dominant disease manifestation of great importance to patients and families, and prolongation of ambulation despite progressive weakness is a major therapeutic goal [McDonald, #53]. The six-minute walk test is safe and reliable tool that evaluates walking endurance and functional capacity in ambulatory patients with neuromuscular diseases, has been used as a primary outcome in DMD clinical trials and has served as the basis for regulatory registration of several drugs [McDonald, #53]. In our study, qualitative measures of adiposity and normalized lower leg IMAT were higher in DMD subjects and elevated fatty infiltration scores for several lower leg muscles, IMAT and SOL lipid fraction correlated negatively with walking endurance. These results indicate that lower leg muscle adiposity measured by MR imaging and spectroscopy can provide an important indicator of functional walking abilities that has the advantage of being objective, non-invasive and independent of patient effort.

Prior 31P-MRS studies have shown decreased PCr/Pi and PCr, increased inorganic phosphate (Pi) and increased pH in gastrocnemius muscle of DMD children [22, 23]. In our study, PCr/Pi of posterior lower leg muscles was significantly lower in DMD children. Because the PCr/Pi ratio is related to the phosphate potential of muscle, it can be used as a measure of bioenergetic reserve and helps assess muscle oxidative metabolism [23]. Lower PCr/Pi ratios indicate impaired oxidative phosphorylation and/or altered ATPase activity, which can occur in muscular dystrophy [23]. Elevated muscle pH has been previously described in DMD [22, 23] and was present in our subjects. It has been postulated that pH increase in DMD may be a response of the muscle cell to dystrophin deficiency, possibly related to regenerative mitogenesis or altered ion transport [22]. However, our study did not reveal significant correlations of PCr/Pi and pH with the Vignos lower extremity functional ratings. The relationship of 31P-MRS parameters with strength and motor function was evaluated in two prior studies, however small sample sizes prevented definite conclusions [24, 25]. Similarly, our 31P-MRS data suggest that in small cohorts of DMD subjects, measures of lower leg muscle high-energy phosphates may not be as sensitive as MR imaging and 1H-MRS measures of adiposity in predicting disease severity.

There were several limitations to our study. Due to time constraints, we did not perform water-sensitive MR imaging pulse sequences that would show muscle edema or inflammation affecting DMD subjects. Although increased water content may affect 1H-MRS lipid fraction measures, we did obtain and separately analyze unsuppressed water spectra from TA and SOL and accounted for variations of water content in our statistical models. Also, the relatively small cohort of DMD subjects at different stages and ages may have played a role in 31P-MRS data not showing significant correlations with functional measures. However, this same cohort provided strong correlations with MR imaging and 1H-MRS measures of adiposity, suggesting these methods may be more sensitive for following disease progression in boys with DMD over time. It seems reasonable to assume that dynamic 31-P-MRS acquisitions (pre- and post-exercise) may be more sensitive in detecting functional decline based on prolonged PCr recovery constants. However, due to the potential impact of exertion prior to our functional measures, we elected not to perform dynamic acquisitions. Further studies using dynamic acquisitions are need to determine sensitivity in predicting functional status in DMD children.

In summary, our results show that despite the potential for pseudohypertrophy and late-stage involvement, lower leg muscles of boys with DMD show a distinct involvement pattern with increased adiposity that correlates with functional status. In small cohorts of DMD subjects, lower leg MR imaging and 1H-MRS studies may help follow disease progression and are sensitive methods by which to monitor non-invasively the severity of muscle involvement.

Acknowledgments

This work was conducted with support from Harvard Catalyst, The Harvard Clinical and Translational Science Center (NIH Award #UL1 RR 025758 and financial contributions from Harvard University and its affiliated academic health care centers). The content is solely the responsibility of the authors and does not necessarily represent the official views of Harvard Catalyst, Harvard University and its affiliated academic health care centers, the National Center for Research Resources, or the National Institutes of Health.

We thank the boys and their families for their dedication and cooperation during this study.

References

1. Bushby K, Finkel R, Birnkrant DJ, et al. Diagnosis and management of Duchenne muscular dystrophy, part 1: diagnosis, and pharmacological and psychosocial management. Lancet Neurol. 2010; 9:77–93. [PubMed: 19945913]
2. Kim HK, Laor T, Horn PS, Racadio JM, Wong B, Dardzinski BJ. T2 mapping in Duchenne muscular dystrophy: distribution of disease activity and correlation with clinical assessments. Radiology. 2010; 255:899–908. [PubMed: 20501727]
3. Schreiber A, Smith WL, Ionasescu V, et al. Magnetic resonance imaging of children with Duchenne muscular dystrophy. Pediatr Radiol. 1987; 17:495–497. [PubMed: 3684364]
4. Liu GC, Jong YJ, Chiang CH, Jaw TS. Duchenne muscular dystrophy: MR grading system with functional correlation. Radiology. 1993; 186:475–480. [PubMed: 8421754]
5. Huang Y, Majumdar S, Genant HK, et al. Quantitative MR relaxometry study of muscle composition and function in Duchenne muscular dystrophy. J Magn Reson Imaging. 1994; 4:59–64. [PubMed: 8148557]
6. Wren TA, Bluml S, Tseng-Ong L, Gilsanz V. Three-point technique of fat quantification of muscle tissue as a marker of disease progression in Duchenne muscular dystrophy: preliminary study. AJR Am J Roentgenol. 2008; 190:W8–12. [PubMed: 18094282]
7. Beenakker EA, Fock JM, Van Tol MJ, et al. Intermittent prednisone therapy in Duchenne muscular dystrophy: a randomized controlled trial. Arch Neurol. 2005; 62:128–132. [PubMed: 15642859]
8. Phoenix J, Betal D, Roberts N, Helliwell TR, Edwards RH. Objective quantification of muscle and fat in human dystrophic muscle by magnetic resonance image analysis. Muscle Nerve. 1996; 19:302–310. [PubMed: 8606693]
9. Sookhoo S, Mackinnon I, Bushby K, Chinnery PF, Birchall D. MRI for the demonstration of subclinical muscle involvement in muscular dystrophy. Clin Radiol. 2007; 62:160–165. [PubMed: 17207699]
10. Vignos PJ Jr, Spencer GE Jr, Archibald KC. Management of progressive muscular dystrophy in childhood. JAMA. 1963; 184:89–96. [PubMed: 13997180]
11. Gallagher D, Kuznia P, Heshka S, et al. Adipose tissue in muscle: a novel depot similar in size to visceral adipose tissue. Am J Clin Nutr. 2005; 81:903–910. [PubMed: 15817870]
12. Provencher SW. Estimation of metabolite concentrations from localized in vivo proton NMR spectra. Magn Reson Med. 1993; 30:672–679. [PubMed: 8139448]
13. Vanhamme L, van den Boogaart A, Van Huffel S. Improved method for accurate and efficient quantification of MRS data with use of prior knowledge. J Magn Reson. 1997; 129:35–43. [PubMed: 9405214]
14. Fleischman A, Kron M, Systrom DM, Hrovat M, Grinspoon SK. Mitochondrial function and insulin resistance in overweight and normal-weight children. J Clin Endocrinol Metab. 2009; 94:4923–4930. [PubMed: 19846731]

15. ATS statement: guidelines for the six-minute walk test. Am J Respir Crit Care Med. 2002; 166:111–117. [PubMed: 12091180]

16. Mayhew JE, Florence JM, Mayhew TP, et al. Reliable surrogate outcome measures in multicenter clinical trials of Duchenne muscular dystrophy. Muscle Nerve. 2007; 35:36–42. [PubMed: 16969838]

17. Cros D, Harnden P, Pellissier JF, Serratrice G. Muscle hypertrophy in Duchenne muscular dystrophy. A pathological and morphometric study. J Neurol. 1989; 236:43–47. [PubMed: 2915226]

18. Jones DA, Round JM, Edwards RH, Grindwood SR, Tofts PS. Size and composition of the calf and quadriceps muscles in Duchenne muscular dystrophy. A tomographic and histochemical study. J Neurol Sci. 1983; 60:307–322. [PubMed: 6886735]

19. Marden FA, Connolly AM, Siegel MJ, Rubin DA. Compositional analysis of muscle in boys with Duchenne muscular dystrophy using MR imaging. Skeletal Radiol. 2005; 34:140–148. [PubMed: 15538561]

20. Arai Y, Osawa M, Fukuyama Y. Muscle CT scans in preclinical cases of Duchenne and Becker muscular dystrophy. Brain Dev. 1995; 17:95–103. [PubMed: 7625556]

21. McDonald CM, Henricson EK, Han JJ, et al. The 6-minute walk test in Duchenne/Becker muscular dystrophy: longitudinal observations. Muscle Nerve. 2010; 42:966–974. [PubMed: 21038378]

22. Kemp GJ, Taylor DJ, Dunn JF, Frostick SP, Radda GK. Cellular energetics of dystrophic muscle. J Neurol Sci. 1993; 116:201–206. [PubMed: 8393092]

23. Younkin DP, Berman P, Sladky J, Chee C, Bank W, Chance B. 31P NMR studies in Duchenne muscular dystrophy: age-related metabolic changes. Neurology. 1987; 37:165–169. [PubMed: 3796830]

24. Hsieh TJ, Jaw TS, Chuang HY, Jong YJ, Liu GC, Li CW. Muscle metabolism in Duchenne muscular dystrophy assessed by in vivo proton magnetic resonance spectroscopy. J Comput Assist Tomogr. 2009; 33:150–154. [PubMed: 19188804]

25. Ikehira H, Nishikawa S, Matsumura K, Hasegawa T, Arimizu N, Tateno Y. The functional staging of Duchenne muscular dystrophy using in vivo 31P MR spectroscopy. Radiat Med. 1995; 13:63–65. [PubMed: 7667509]

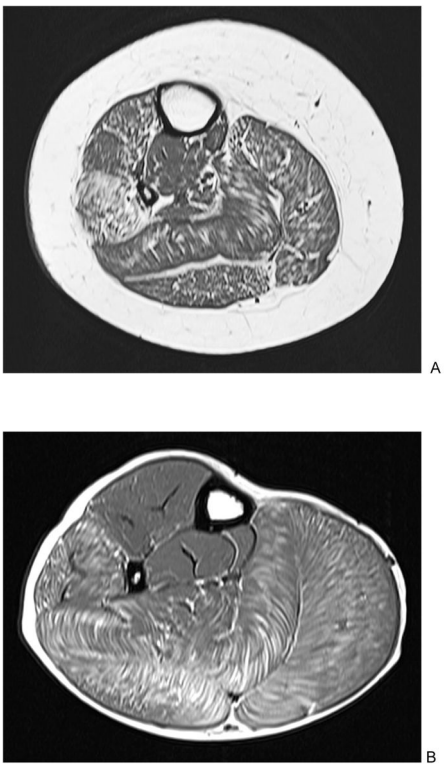

Figure 1.
T1-weighted axial images of the right lower leg in two boys with DMD aged 14 (A) and 10 (B) years. There are varied degrees of muscle fatty infiltration, with predominant involvement of peroneal, soleus and gastrocnemius muscles, and relative sparing of tibialis posterior muscle.

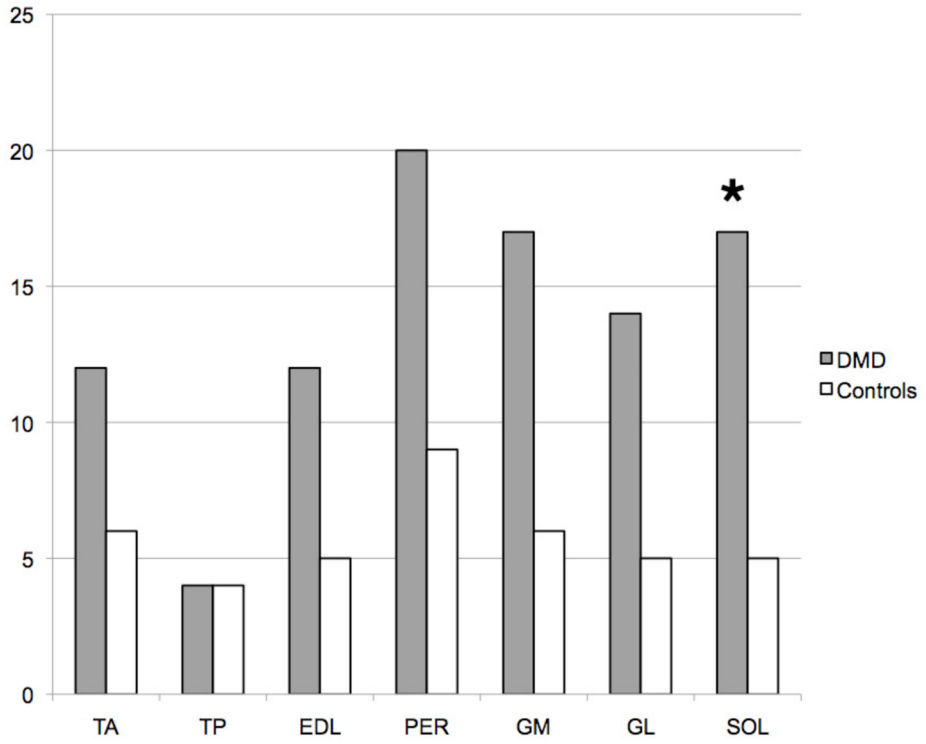

Figure 2.
Bar chart showing the cumulative total fatty infiltration scores for lower leg muscles of DMD (dark) and control groups (white) on T1-weighted images. TA, tibialis anterior; TP, tibialis posterior; EDL, extensor digitorum longus; PER, peroneus muscles; GM and GL, gastrocnemius medialis and lateral, respectively; SOL, soleus. *, P = 0.01 when comparing DMD to control subjects.

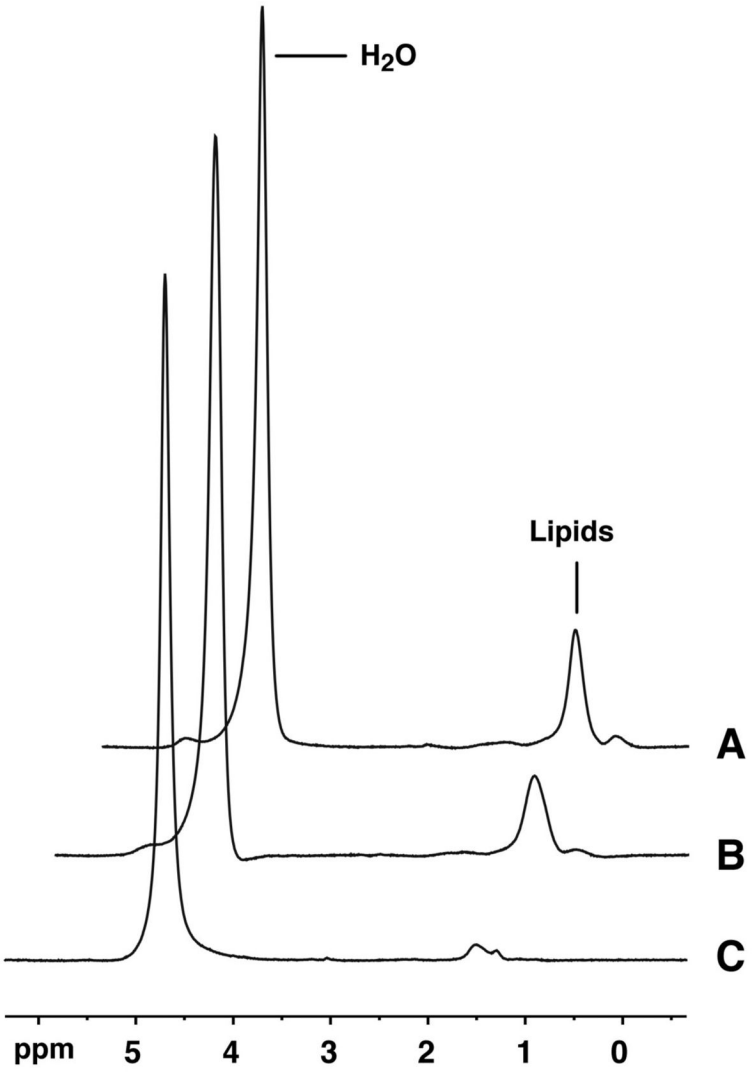

Figure 3.
Unsuppressed 1H-MRS spectra of soleus muscle in 14-year old (A) and 10-year-old (B) boys with DMD, compared to a 12-year old control subject (C) show substantially increased lipid resonances in DMD subjects. Subjects (A) and (B) are the same as in Figure 1, respectively.

Table 1

Vignos lower extremity functional rating scale for DMD [10].

Score	Definition
1	Walks and climbs stairs without assistance.
2	Walks and climbs stairs with aid of railing.
3	Walks and climbs stairs slowly with aid of railing (over 25 sec for eight standard steps).
4	Walks unassisted and rises from chair but cannot climb stairs.
5	Walks unassisted but cannot rise from chair or climb stairs.
6	Walks only with assistance or walks independently with long leg braces.
7	Walks in long leg braces but requires assistance for balance.
8	Stands in long leg braces but unable to walk even with assistance.
9	Is in wheel chair. Elbow flexors more than antigravity.
10	Is in wheel chair or bed. Elbow flexors less than antigravity.

Table 2

MR imaging, 1H- and 31P-MRS data for DMD and control groups

Parameter	DMD group	Control group	*P-value*
MR imaging			
IMAT/mCSA	0.16 ± 0.09	0.08 ± 0.05	**0.04**
IMAT (cm^2)	9.36 ± 10.4	4.73 ± 3.4	0.25
mCSA (cm^2)	52.1 ± 26.6	61.5 ± 17.3	0.41
1H-MRS			
TA LF (%)	9.2 ± 12.6	2.5 ± 2.0	**0.02** [a]
SOL LF (%)	28.4 ± 24.8	7.4 ± 4.0	**0.003**[a]
31P-MRS (anterior lower leg)			
PCr (AU)	274.8 ± 74.9	332.0 ± 38.2	0.07
Pi (AU)	74.1 ± 28.2	65.9 ± 26.8	0.56
PCr/Pi	4.2 ± 1.9	5.6 ± 1.6	0.14
pH	7.09 ± 0.03	7.03 ± 0.02	**0.0003**
31P-MRS (posterior lower leg)			
PCr (AU)	254.9 ± 66.8	290.2 ± 21.7	0.17
Pi (AU)	67.9 ± 18.7	59.4 ± 13.5	0.30
PCr/Pi	3.8 ± 0.8	5.1 ± 1.2	**0.02**
pH	7.12 ± 0.05	7.09 ± 0.03	0.13

[a] ANCOVA after log conversion to approximate a normal distribution and controlling for unsuppressed water concentration.

IMAT/mCSA, intramuscular adipose tissue normalized to total muscle cross sectional area; LF, lipid fraction; TA, tibialis anterior; SOL, soleus; AU, arbitrary units.